

# Allotropic Modifications of Cobalt upon Chemical Deposition

A. V. Chzhan<sup>a, b, \*</sup>, S. A. Podorozhnyak<sup>a</sup>, V. K. Mal'tsev<sup>c</sup>, I. N. Krayukhin<sup>a</sup>, and G. S. Patrin<sup>a, c</sup>

<sup>a</sup> Siberian Federal University, Krasnoyarsk, 660041 Russia

<sup>b</sup> Krasnoyarsk State Agrarian University, Krasnoyarsk, 660049 Russia

<sup>c</sup> Kirensky Institute of Physics, Krasnoyarsk Scientific Center, Siberian Branch, Russian Academy of Sciences, Krasnoyarsk, 660036 Russia

\*e-mail: avchz@mail.ru

Received March 24, 2020; revised July 7, 2020; accepted August 25, 2020

**Abstract**—The effect of the solution acidity on the crystal structure of cobalt during its chemical deposition is reported. It has been shown using the structural and magnetic examination and nuclear magnetic resonance study that the change in the working solution acidity leads to deposition of cobalt with different allotropic modifications in the nearest environment: the hcp type in the small (up to ~8.5) pH region and the fcc type in the large (over ~8.5) pH region. The formation of these cobalt modifications is attributed to the size effects caused by a decrease in the particle size with increasing pH.

**Keywords:** Co–P thin magnetic films, chemical deposition, nuclear magnetic resonance, allotropic modifications of Co

**DOI:** 10.1134/S1063783421010054

## 1. INTRODUCTION

The technique of electrodeless or currentless chemical deposition of metals attracts by the possibility of creating films with a high degree of homogeneity and setting various characteristics of samples by choosing the conditions of chemical reactions, for example, deposition temperature or acidity of a reducing medium. In view of this, the use of chemical technology for obtaining magnetic films from alkaline hypophosphite solutions is of undoubted interest. The most well-known application of this technology is fabrication of cobalt films with the phosphorus addition in the course of appropriate chemical reactions [1]. At the low phosphorus content, such films exhibit the high saturation magnetization similar to that of unalloyed cobalt [2]. In addition, the use of chemical technology for obtaining Co–P films attracts attention by the fact that the magnetic characteristics of the films can be qualitatively changed by choosing the deposition conditions. In particular, by changing the acidity of working solutions, one can create both the high- and low-anisotropy samples with significantly different coercivities  $H_C$  [3]. Therefore, the chemically deposited cobalt films have a great potential for application, e.g., in magnetic memory [4, 5] and various control or readout devices [6, 7]. Despite a great number of studies on the effect of the solution acidity on the structural and magnetic properties of chemically deposited cobalt films [8–11], to date, there has been a lack of information on the cobalt crystal lattice modifications depending on the constituent grain size.

In this study, basing on the results of structural and magnetic investigations and nuclear magnetic resonance (NMR) study, it is shown that a change in acidity of the working solution leads to deposition of cobalt in different allotropic modifications in the nearest environment: the hcp type in the small (up to ~8.5) pH region and the fcc type in the large (over ~8.5) pH region. The formation of these cobalt allotropes is attributed to the size effects caused by a decrease in the particle size with increasing pH.

## 2. EXPERIMENTAL

The working liquor was an aqueous solution of cobalt sulfate  $\text{CoSO}_4 \cdot 7\text{H}_2\text{O}$  (15 g/L), sodium hypophosphite  $\text{NaH}_2\text{PO}_2 \cdot \text{H}_2\text{O}$  (10 g/L), and sodium citrate  $\text{Na}_3\text{C}_6\text{H}_5\text{O}_7$  (25 g/L). A required pH value was specified by adding alkaline reagents, which were sodium bicarbonate  $\text{NaHCO}_3$  or sodium hydroxide  $\text{NaOH}$ , in different concentrations. The solution acidity was detected with a pH-150MИ pH meter accurate to  $\pm 0.05$ . The deposition was performed at a temperature of  $\sim 100^\circ\text{C}$  in a magnetic field of  $H \approx 3 \text{ kOe}$  for 3 min onto coverslip substrates subjected to the cleaning, sensibilization, and activation procedures used for chemical metallization of dielectrics [12]. During deposition, a magnetic field was applied parallel to the substrate plane. The easy axis of the induced magnetic anisotropy of the obtained films was co-directed with the applied magnetic field.

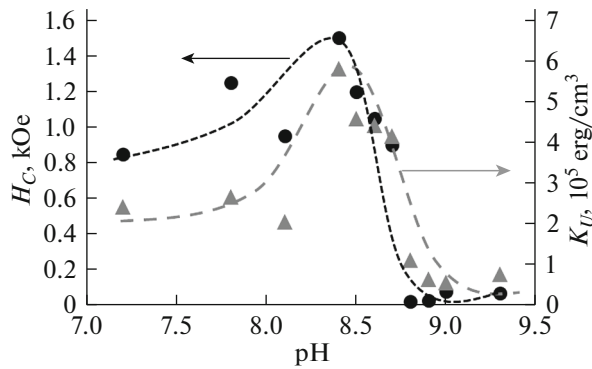


Fig. 1. Coercivity and induced magnetic anisotropy constant of the Co–P films vs pH of the deposition solutions.

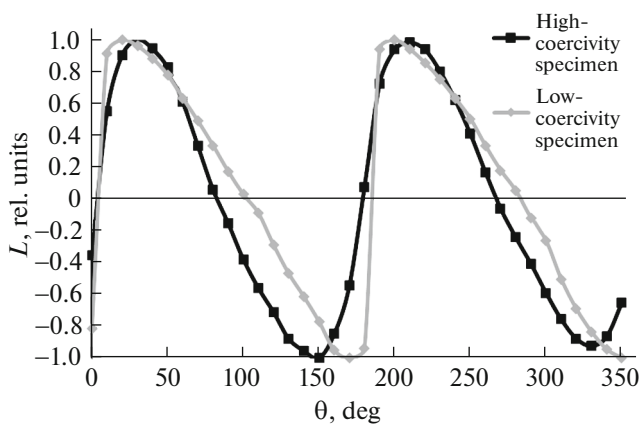


Fig. 2. Torque curves for the high- and low-coercivity samples.

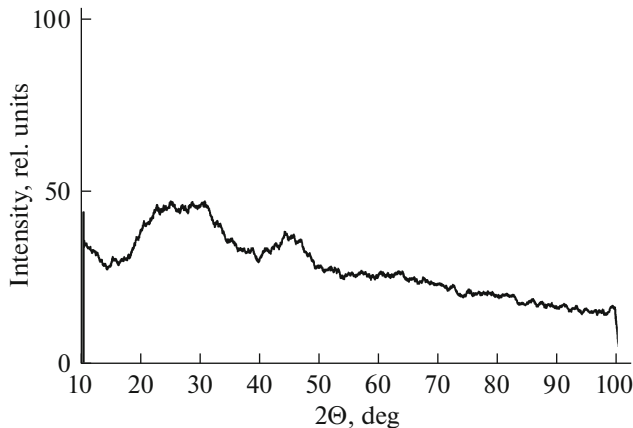


Fig. 3. X-ray diffraction pattern of the low-coercivity film obtained at pH  $\sim$  8.9.

The film microstructure was studied by transmission electron microscopy (TEM) on a Hitachi HT-7700 microscope equipped with a Bruker X-Flash

6T/60 energy dispersive detector. The coercivity and the induced anisotropy constant were determined using, respectively, the meridional Kerr effect and a torque magnetometer in a dc magnetic field of 10 kOe applied parallel to the film plane at room temperature.

The NMR signals were measured on a standard spin echo device in the range of 150–250 MHz.

### 3. RESULTS

Figure 1 shows the dependence of induced anisotropy constant  $K_U$  and coercivity  $H_C$  of the Co–P films on pH of their deposition solutions.

In the low (7.2–8) pH region, the  $K_U$  value is  $\sim 2.5 \times 10^5$  erg/cm<sup>3</sup>. The pH growth leads to an increase in the anisotropy and, in the pH region around 8.5  $K_U$ , the anisotropy constant attains  $\sim 6 \times 10^5$  erg/cm<sup>3</sup>. A further increase in the acidity leads to the abrupt (by an order of magnitude)  $K_U$  drop down to  $5 \times 10^4$  erg/cm<sup>3</sup>. As the pH value increases to  $\sim 8.5$ , the  $H_C$  value grows from  $\sim 1$  kOe to  $\sim 1.5$  kOe and, then, with a further increase in pH, decreases almost stepwise to several oersted. Both the high- and low-coercivity samples exhibit the uniaxial anisotropy with four maxima in the torque curves upon film rotation by 360° (Fig. 2). In the low-coercivity samples, a sharp change in the torque around 0 and 180°, which correspond to the easy axis direction, is due to the fact that, in these films, the anisotropy field  $H_K$  is much higher than  $H_C$  [3].

The induced anisotropy in the low- and high-coercivity samples is governed by different physical mechanisms. In the first case, this is the ordering of atomic pairs [3]. The origin of the induced anisotropy in the high-coercivity samples is still unclear and needs further investigations.

In [13], based on the X-ray diffraction data, we showed that the crystal structure of the investigated samples deposited at pH < 8.5 contains a pronounced hexagonal cobalt phase, which determines their high coercivity. In addition, it was found that the transition of the films to the low-coercivity state in the pH range of >8.5 occurs together with the structural changes. The X-ray diffraction patterns of the low-coercivity samples (Fig. 3) have diffuse halos near the main peaks of both the fcc and hcp cobalt crystal lattice located in the range of 40°–50°, which is typical of nanocrystalline materials without long-range order.

The sensitivity of X-ray diffraction analysis is insufficient to obtain data on the nearest environment of cobalt atoms in thin films with fine grains. Therefore, to study such samples in more detail, we additionally used a technique based on the analysis of the NMR spin echo spectrum [14]. It is well-known that the NMR spin echo signal amplitude  $A_E$  is determined by magnetic susceptibility  $\chi$  of the sample, which is

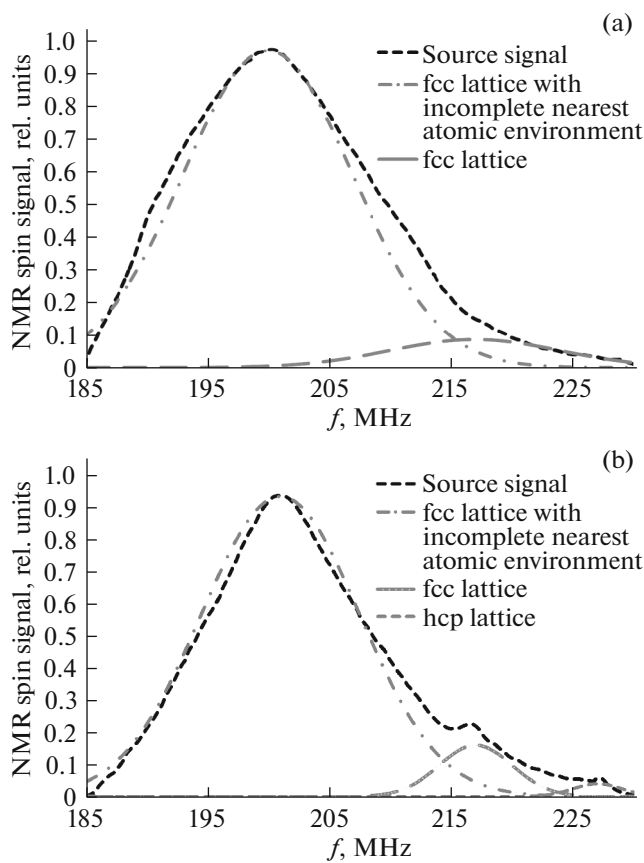


**Fig. 4.** Spin echo spectrum of the samples obtained at pH (a)  $\sim 9.15$  and (b)  $\sim 8.9$ .

inversely proportional to the magnetic anisotropy field:  $A_E \sim 1/H_K$ .

For this reason, the NMR method was used to study only the low-anisotropy samples. To determine the contributions of different structural phases to the NMR signals, the integral curve was decomposed into normal distribution components (Fig. 4).

The NMR spin echo absorption spectra are broad lines in the range of 185–230 MHz with a diffuse maximum near  $\sim 200$  MHz, the signal intensity drop to zero in the left-hand low-frequency portion, and characteristic absorption features in the right-hand high-frequency portion. The main absorption maximum corresponds to incomplete filling of the first coordination sphere (11 instead of 12) in the nearest environment of cobalt atoms forming the fcc-type short-range order. This effect can be related to defects in the cobalt crystal lattice, diamagnetic substitution of a phosphorus atom for one cobalt atom, edge/surface effects, and uncompensated bonds on the crystallite surface. The side absorption maxima at frequencies of 216 and 227 MHz correspond to the high-frequency absorption by cobalt nuclei arranged in the short-range order of the fcc and hcp types, respectively. For the sample corresponding to Fig. 4b, the peak at a frequency of

216 MHz is more intense, while for the sample corresponding to Fig. 4a, this peak is more diffuse, which is indicative of stronger structural disordering of the nearest environment of atoms in the fcc packing. In addition, in Fig. 4b, one can see an additional peak at a frequency of 227 MHz, which corresponds to the signal from the nearest environment of cobalt atoms arranged according to the hcp type.

#### 4. DISCUSSION

An increase in the pH value of the working solution leads to a decrease in the film grain size, which is clearly reflected in the surface morphology (Fig. 5). The characteristic inhomogeneity size determined by the AFM technique (Fig. 6a) agrees well with the change in the crystallite size determined by the TEM technique (Fig. 6b). In both cases, we observe a monotonic, almost linear decrease in the size of structural elements with increasing pH.

As is known, in cobalt, the size of particles correlates with their crystal structure, which is caused by the different particle size dependences of the free energy of the  $\alpha$  and  $\beta$  phases. For fine particles with sizes of  $d < 20$  nm, the fcc structure ( $\beta$  phase) is preferred; for coarse particles with  $d > 40$  nm, the hcp structure ( $\alpha$  phase) is preferred; and in the intermediate size range, the phase mixture exists [15, 16]. The formation of a certain phase modification is determined by the competing contributions of the bulk and surface energies; the ratio between them depends on the particle size and is different for the  $\alpha$  and  $\beta$  phases.

The above-mentioned features of cobalt explain well the transformation of the crystal structure of its particles in the films under study. It follows from the presented data that the films obtained in the low-pH solution consist of coarse crystallites ( $d \sim 70$  nm); for such particles, the  $\alpha$  phase of Co is stable, which was observed in the experiments. As the pH value increases, the particle size decreases and the pH values higher than  $\sim 8.5$  lead to the instability of the hexagonal phase and the onset of packing of atoms in the fcc-type structures in the nearest environment of cobalt. At the initial stage of the transition, there is a mixture of these phases with the dominance of hcp cobalt, which is reflected in the magnetic characteristics of the samples. A sharp decrease in the  $K_U$  value around pH  $\sim 8.75$  shows that, at such an acidity of the solution, the transition from the  $\alpha$  to  $\beta$  phase is completed and the magnetic properties of the film are determined by the  $\beta$  phase of Co. The diffuse transition of the particle structure from the hcp to fcc type can result from scattering of the size of particles, which leads to their phase inhomogeneity. With a further increase in the acidity, the  $\alpha$  phase of cobalt is suppressed and the substance passes mainly to the short-range ordering of the fcc type with the incomplete environment.

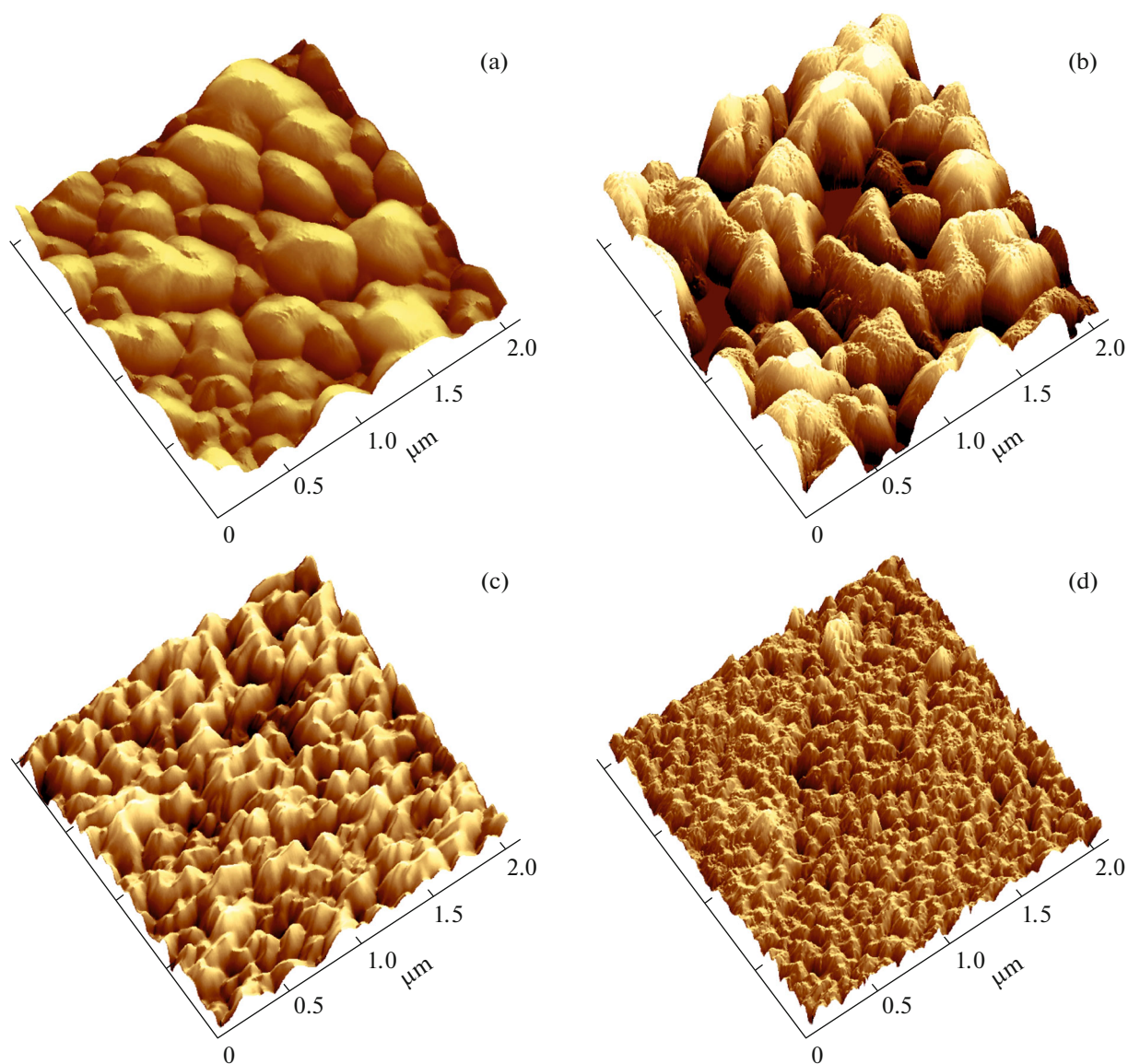


**Fig. 5.** AFM image of the surface of the films obtained at pH = (a) 7.2, (b) 8.7, (c) 8.9, and (d) 9.3.

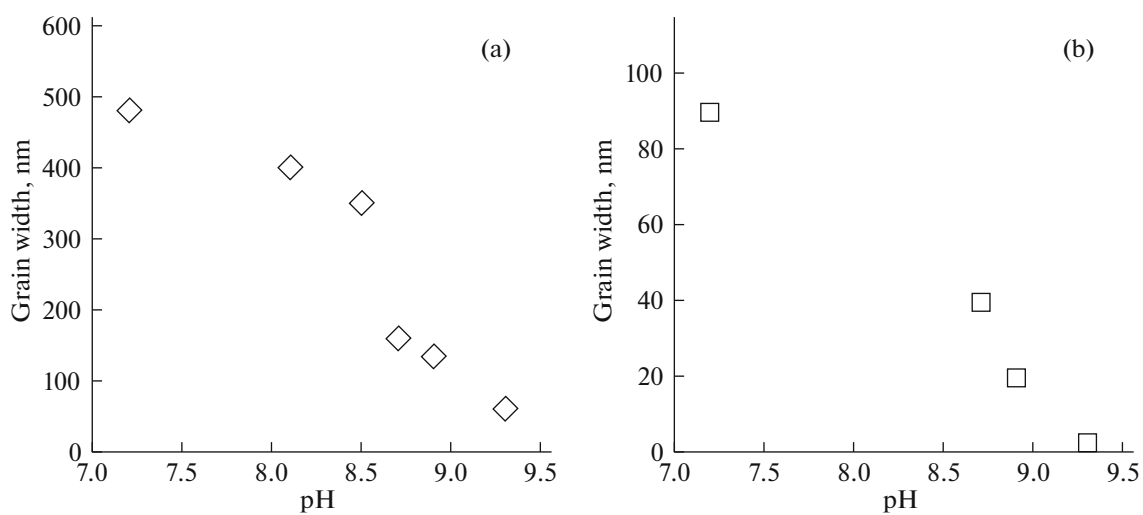


**Fig. 6.** (a) Average size of surface inhomogeneities (AFM) and (b) average grain size (TEM) vs pH.

## 5. CONCLUSIONS

The results obtained showed that a decrease in the characteristic crystallite size caused by an increase in the pH value of the solutions during chemical deposition of the Co–P films leads to the allotropic transformations of the nearest environment of cobalt from the hcp type in the small (up to ~8.5) pH region to the fcc type in the large (over ~8.5) pH region. Such crystal structure transformations, in addition to the effects caused by the random anisotropy [13, 17], are reflected in the magnetic properties of the investigated films, including their induced anisotropy and coercive force.

## ACKNOWLEDGMENTS

We are grateful to V.G. Myagkov for help in the measurements of the induced magnetic anisotropy constants.

## FUNDING

This study was supported in part by the Russian Foundation for Basic Research, project no. 18-02-00161-a.

## CONFLICT OF INTEREST

The authors declare that they have no conflicts of interest.

## REFERENCES

1. G. O. Mallory and J. B. Hajdu, *Electroless Plating: Fundamentals and Applications* (Am. Electroplaters Surf. Finishers Soc., Orlando, 1990).
2. A. V. Chzhan, S. A. Podorozhnyak, G. S. Patrin, R. Yu. Rudenko, and V. V. Onufrienok, *J. Phys: Conf. Ser.* **1389**, 012116 (2019).
3. A. V. Chzhan, S. A. Podorozhnyak, M. N. Volochaev, and G. S. Patrin, *EPJ Web Conf.* **185**, 03012 (2018).
4. E. L. Nicholson and M. R. Khan, *J. Electrochem. Soc.* **133**, 2342 (1986).
5. M. Mirzamaani, L. Romankiw, C. McGrath, J. Mahlke, and N. C. Anderson, *J. Electrochem. Soc.* **135**, 2813 (1988).
6. H. Wang, Z. Du, L. Wang, G. Yu, and F. Zhu, *J. Univ. Sci. Technol. Beijing* **15**, 618 (2008).
7. H.-C. Wang, G.-H. Yu, J.-L. Cao, and L.-J. Wang, *Sens. Actuators, A* **165**, 216 (2011).
8. U. Admon, A. Bar-Or, and D. Treves, *J. Appl. Phys.* **44**, 2300 (1973).
9. L. Nianduan, C. Jian, and L. Liangliang, *Surf. Coat. Technol.* **206**, 4822 (2012).
10. L. A. Chekanova, R. S. Iskhakov, G. I. Fish, R. G. Khlebopros, and N. S. Chistyakov, *JETP Lett.* **20**, 31 (1974).
11. A. V. Chzhan, T. N. Patrusheva, S. A. Podorozhnyak, V. A. Serezhkin, and G. N. Bondarenko, *Bull. Russ. Acad. Sci.: Phys.* **80**, 692 (2016).
12. K. M. Vansovskaya, *Metal Coatings Applied by Chemical Methods* (Mashinostroenie, Leningrad, 1985) [in Russian].
13. A. V. Chzhan, S. A. Podorozhnyak, M. N. Volochaev, G. N. Bondarenko, and G. S. Patrin, *Phys. Solid State* **59**, 1440 (2017).
14. V. K. Mal'tsev, G. I. Fish, and V. I. Tsifrinovich, *Fiz. Met. Metalloved.* **52**, 439 (1981).
15. H. Sato, O. Kitakami, T. Sakurai, Y. Shimada, Y. Otani, and K. Fukamichi, *J. Appl. Phys.* **81**, 1858 (1997).
16. O. Kitakami, H. Sato, Y. Shimada, F. Sato, and M. Tanaka, *Phys. Rev. B* **56**, 13849 (1997).
17. G. Herzer, in *Handbook of Magnetic Material* (Elsevier Science B. V., North Holland, 1997), p. 415.

*Translated by E. Bondareva*